



## FEM ANALYSIS OF STRUCTURAL PERFORMANCE DETERIORATION OF RC ELEMENTS SUBJECTED TO SEISMIC REVERSED CYCLIC SHEAR

Hiroshi NOGUCHI<sup>1</sup> and Takashi KASHIWAZAKI<sup>2</sup>

### SUMMARY

In this study, the models under monotonic loading of three-dimensional FEM analysis program which developed by Noguchi and Uchida(1998)[1] are expanded to the models under reversed cyclic loading. Furthermore, the orthogonal fixed cracking model is developed in order to elucidate the stress transfer mechanisms, and establish three-dimensional FEM analytical technique of reinforced concrete members under reversed cyclic loading. Columns and beam-column joints are analyzed in order to verify the revised analytical models.

### 1. INTRODUCTION

In the seismic design based on the inelastic displacement concept, specific necessary lateral loads, story drifts and structural members deformations should be kept within the design limitation during the earthquake in order to ensure the seismic performance. The correct analytical predication of the energy absorbed by structural elements is necessary to assure this design concept. In the FEM analysis of RC elements, the target of the analytical model is to simulate the hysteretic behavior of the structural elements correctly. In this study, more realistic analysis models such as a transition hysteresis model for concrete stress-strain relationships especially in tension-compression regions, an orthogonal fixed cracking model, and a hysteresis model for shear characteristics of cracked concrete, considering deterioration and fracture mechanics, are incorporated into the three-dimensional non-linear FEM analysis programs developed by the authors. The characteristics of the behavior of reinforced concrete elements under cyclic shear, such as the tangent stiffness for unloading and reloading, slip stiffness, residual strain and the deterioration, can be simulated more precisely. The revised three-dimensional FEM program, using revised concrete and reinforcement hysteresis models considering the deterioration of the materials under cyclic shear, is applied to RC columns and beam-column joints in order to verify the revised analytical models. The analytical results gave a correct estimation of unloading and reloading hysteresis shapes of load-deflection curves and residual displacement as compared with the test results. The revised FEM analytical program will be useful to clarify the three-dimensional mechanisms of strength degradation of

---

<sup>1</sup>Professor, Councilor, Chiba University, Chiba, Japan. Email: [noguchi@faculty.chiba-u.jp](mailto:noguchi@faculty.chiba-u.jp)

<sup>2</sup>Research Associate, Chiba University, Chiba, Japan. Email: [kashiwa@faculty.chiba-u.jp](mailto:kashiwa@faculty.chiba-u.jp)

structural elements subjected to two-directional cyclic shear and flexure and also investigate the effects of the strength degradation of structural elements on the structural performance of RC structural systems.

## **2. OUTLINE OF ANALYTICAL METHOD, MATERIAL MODELS AND DEFINITION OF ACCUMULATED CONSUMPTION STRAIN ENERGY**

### **2.1 Cyclic Hysteresis Rules of Concrete and Reinforcement**

In this study, according to the knowledge provided by the previous experiment about cyclic behavior of concrete and the models proposed by Naganuma & Ohkubo (2000)[2], the cyclic hysteresis loops including unloading and reloading curves in tension and compression regions and the region between tension and compression are defined as shown in Figs. 1-4 using multi-curves. They can simulate cyclic hysteresis behavior of concrete very well and also contribute to removing the difficulty of the convergence in solving the equations. And the cyclic hysteresis of reinforcement is defined as shown in Fig. 5 by using the Menegotto-Pinto model proposed by Ciampi & Paolo (1982) [3].

The examples of the proposed analytical hysteresis loops are shown in Fig.6 as compared with the corresponding compressive stress-strain curves obtained in the previous tests by Karsan & Jirsa (1969) [4] and Tanigawa & Kosaka (1978) [5]. As the reloading curve was represented with the straight lines, the area of the analytical hysteresis loops is a little small as the strain at the unloading point became high-levelled. Through the comparison with Tanigawa's test result (1978) in Fig.6, the stress degradation from cyclic loading with constant strain can be represented. But the degradation level is smaller in the analysis results as compared with the test results. The relationships between the reduction ratio of the upper limit stress and the number of cyclic loading with constant compressive strain in this model are shown in Fig. 7. The reduction of the upper limit stress at each loading cycle becomes more remarkable as the number of loading cycle or the compressive strain increases. The reduction ratio tends to converge nearly at the tenth cycle independently of the magnitude of the upper limit strain.

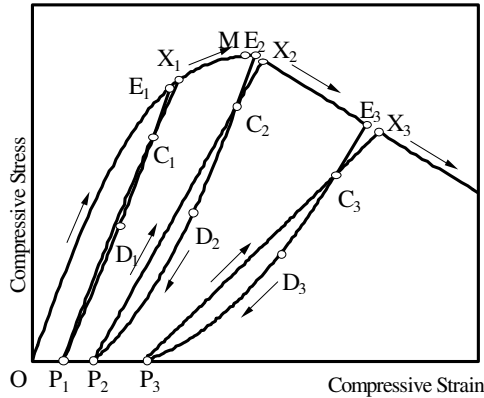
### **2.2 Damage Model of RC Elements**

As for concrete, 8-nodal isoparametric elements are used. The tension stiffening effect in the orthogonal direction of a crack depending on bond is represented by the Sato & Shirai's equation (1978) [6] as shown in Fig. 3. As for the shear stiffness along the crack surface, the Ihzuka & Noguchi's model (1992) [7], which substitutes the dowel stiffness of reinforcement for the equivalent stiffness of concrete, is superimposed on the concrete, the Kupfer & Gerstle's model (1973) [8] is used. The directions of the principal axes are the same as the directions of principal stress before cracking of concrete. When the concrete element cracks, the principal axes are fixed and do not change again. These directions are calculated by the Mohr's stress circle at each loading step. As for the compressive strength in the direction parallel to the crack, the Noguchi & Ihzuka's equation (1992) that consider the reduction factor of the compressive strength with parameters such as crack width (tensile strain) and uni-axial compressive strength is used. As for the nonlinear behavior characteristics of cracked concrete elements, tension stiffening, the shear stiffness along the crack surface and the constitutive law of the shear transfer proposed by Al-Mahaidi(1979) [9] are used.

### **2.3 Crack Models**

The rotating crack model and fixed crack model are used to calculate the shear stiffness along the crack surface. In the rotating crack model, which allows the the revolution of the principal axis, the directions

- Order : O·E·C·D·P·C·X
- P. E : Unloading Point
- P. C : Common Point ( $\sigma_c = 5/6\sigma_E$ )
- P. D : Stiffness Change Point ( $\sigma_D = 1/2\sigma_E$ )
- P. P : Compression Side Residual Strain Point (Suggestion Type of Karsan & Jirsa (1969))
- P. X : Envelope Curve Recovering Point
- P. M : Maximum Strength Point



- P. O-M : Compression Envelope Curve (Type of Saenz (1964))
- P. E-D : The Straight Having the Slope According to a Compressive Strain (by Naganuma & hkubo(2000))
- P. D-P : Second curve
- P. P-X : Straight

Fig 1. Hysteresis Model of Compression Area of Concrete

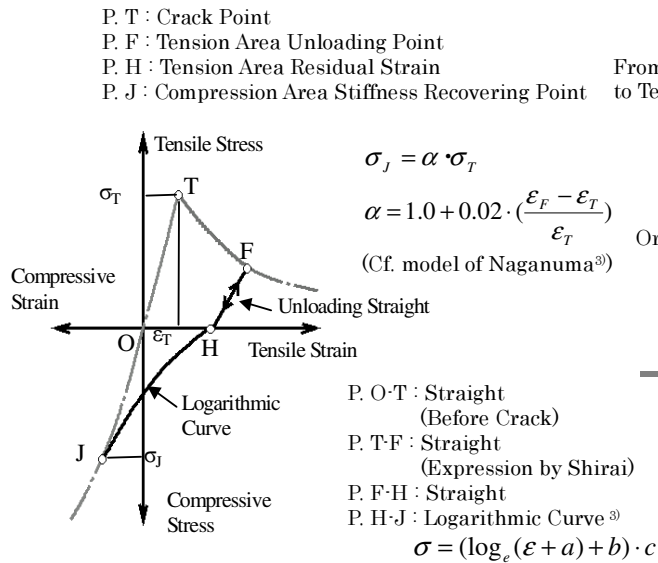


Fig 3. Hysteresis Model of Tension Area of Concrete

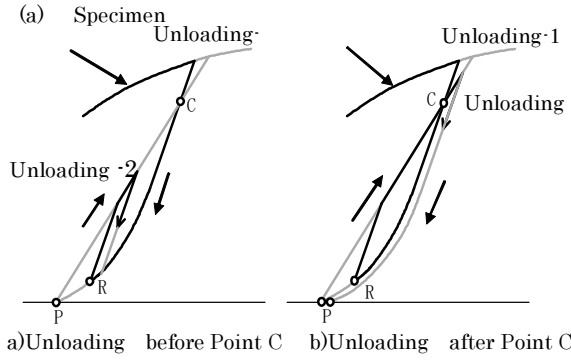
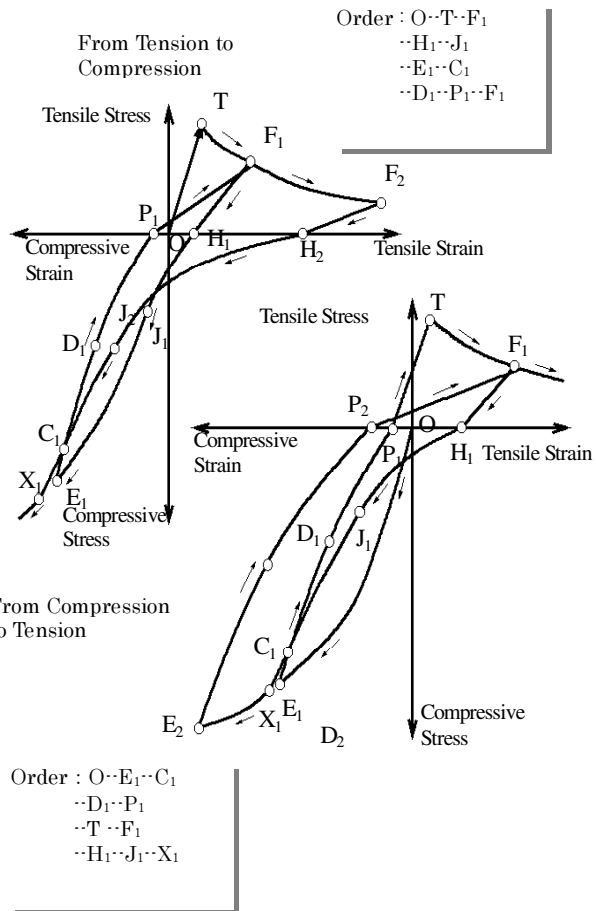


Figure 2. Unloading/Reloading Rule in Compression Area



- Order : O·T·F1
  - H1·J1
  - E1·C1
  - D1·P1·F1
- From Tension to Compression
- P. T : Crack P Point
  - P. F : Tensile Side Unloading Point
  - P. J : Compression Side Envelope Curve Recovery Point of stiffness
  - P. E : Compression Side Unloading Point
  - P. P : Residual Strain Point
  - P. C : Common Point
- From Compression to Tension
- Order : O·E1·C1
  - D1·P1
  - T·F1
  - H1·J1·X1

Figure 4. History between Compression and Tension of Concrete

of the principal axes change prestep because of the revolution of the principal stress or strain. The crack

always occurs in the most weak direction of the concrete element. Because there are only two or three non orthogonal cracks occur in one position in fact, the analytical results using rotating crack model may be lower than the tests on strength and stiffness. In this study, the fixed orthogonal crack model is introduced to the three-dimensional FEM analysis program. With this model, the principal axes are fixed after the crack occurs, and only three orthogonal cracks are allowed in all.

### 2.4 Consumption Strain Energy of RC Elements

As for the ductility of RC structures and members, it is known that the ductility changes largely with the load history. According to the reversed cyclic loading experience of structural members, even in the loading of fixed displacement, the decrease of stiffness and strength is observed along with increase of cyclic loading number. Then, from the viewpoint of energy, the attempts to appraise the seismic safety of the structure were done recently. In the research by Uomoto and others(1993) [11], the RC simple beam with flexural failure mode was tested. In spite of differences of loading displacement and loading patterns, the specimens failed at the identical cumulative consumption energy quantity. As for the same failure mode, the possibility of presuming numbers of reversed cyclic loads up to the failure by the accumulated consumption energy was shown.

In the research by Suzuki and others(1994) [12], the technique of presuming the degree of damage was suggested as an index by the accumulated consumption energy quantity. Furthermore, the application to the seismic design was tried as the scale of the reliability of RC structures.

In the research, it is considered that the accumulated consumption strain energy is the quantity which corresponds to the degree of damage. For grasping detailed damage process

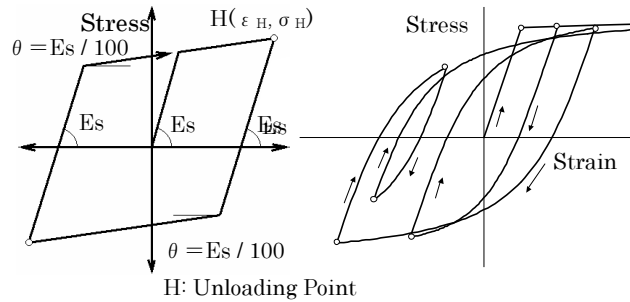


Fig 5. Hysteresis Rule of Reinforcing Bars  
(Left) Traditional Bi-Linear  
(Right) Menegotto-Pinto Model

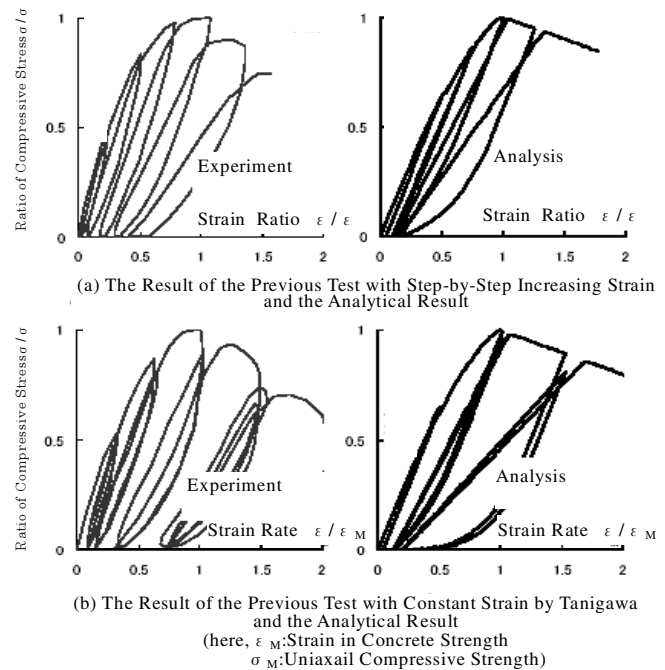


Fig 6. Test and Analyses under Compression Cyclic Loading

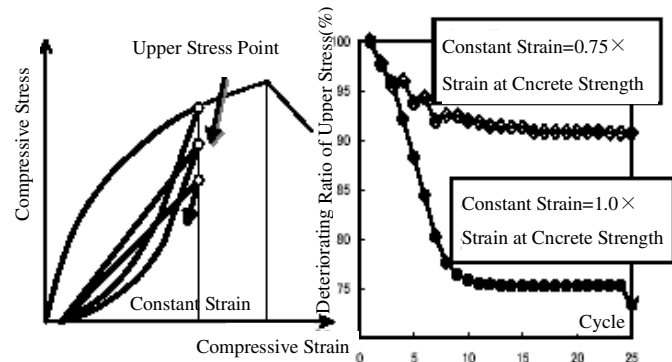


Fig 7. Deterioration of Upper Stress under Compression Cyclic Loading

analytically up to the final stage of RC structures. The quantitative evaluation by accumulated consumption strain energy of concrete elements, hoop elements and the other elements of the specimen is important. Furthermore, it becomes possible to understand the concentricity of the damage in the specimen (by displaying the accumulated consumption energy of the RC in the contour figure).

### 3. THREE-DIMENSIONAL NONLINEAR FEM ANALYSIS OF RC COLUMNS SUBJECTED TO THE BIAxIAL LATERAL LOADINGS

RC columns with an axial load and biaxial lateral loadings, have three dimensional stress state. Some experimental researches on the shear failure of the RC columns under biaxial lateral of stress state have been done before by researchers such as Yoshimura and others(1998) [13], but, the number of analytical researches is very few. In this study, the strength, deformation characteristic condition and failure criterion curve of the column subjected to the biaxial lateral loading, are studied by using three dimensional

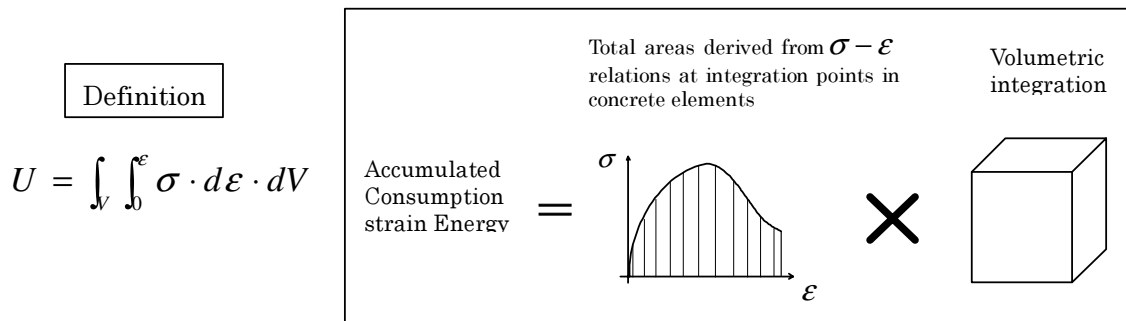


Fig.8 Definition of Accumulated Consumption strain Energy

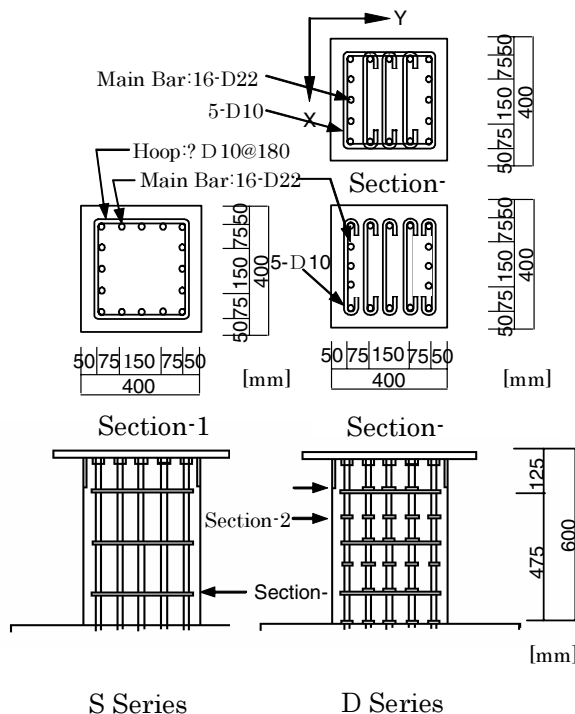


Fig.9 Bar Arrangement of Column Specimens

Table.1 Properties of Column

Specimen	Horizontal Load to Y Direction	Axial Load	Axial Load Ratio	Lateral Reinforcement Ratio in X Direction	Lateral Reinforcement Ratio in Y Direction
S00	0	150tf (1470kN)	0.366	$P_{wx}=0.2\%$	$P_{wy}=0.2\%$
S15	15tf (147kN)				
S25	25tf (245kN)				
S35	35tf (343kN)				
D00	0			$P_{wx}=1.0\%$	
D15	15tf (147kN)				
D25	25tf (245kN)				
D35	35tf (343kN)				

Table.2 Material Properties

Concrete	Comp. Strength	Strain at Comp. Strength	Young's Modulus	
	25.1MPa	0.27%	20.7GPa	
Reinforcement	Yield stress	Maximum Stress	Yield Strain	Young's Modulus
	D10	365M Pa	526M Pa	0.21%
D22	392M Pa	581M Pa	0.20%	194G Pa

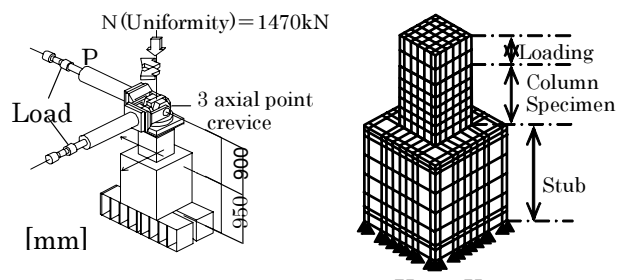


Fig.10 Loading Method Fig.11 Finite Element Idealization

non-linear FEM analysis as compared with the test results. Furthermore, the stress condition, the failure development process are studied.

### 3.1 Outline of Analysis

The three dimensional non-linear FEM analyses were carried out on the RC columns tested by Yosimura and others. The specimens' size and bar arrangement are shown in Fig.9, and the specimens' details are shown in Table.1. The material properties are shown in Table.2, and the Loading method is shown in Fig.10. As for the loading sequence, the fixed axial force was loaded first, and then the fixed horizontal force is loaded in Y direction. While the fixed axial load and fixed horizontal load in Y direction were kept, X directional force was loaded with displacement-controll. Finite element idealization is shown in Fig.11.

### 3.2 Analytical Results

Relationship of X directional horizontal force and deformation of each specimen is shown in Fig.12. The white circle in the figure is the point that the maintenance of Y directional fixed horizontal force or fixed axial force in the experiment became impossible (limit point of loading). From both the analysis and experiment, the X directional maximum strength was small when the Y directional horizontal force was large. The analytical maximum strength of each specimen became larger than the experimental one. This may come from that there is no slip between concrete and reinforcement elements in the analysis.

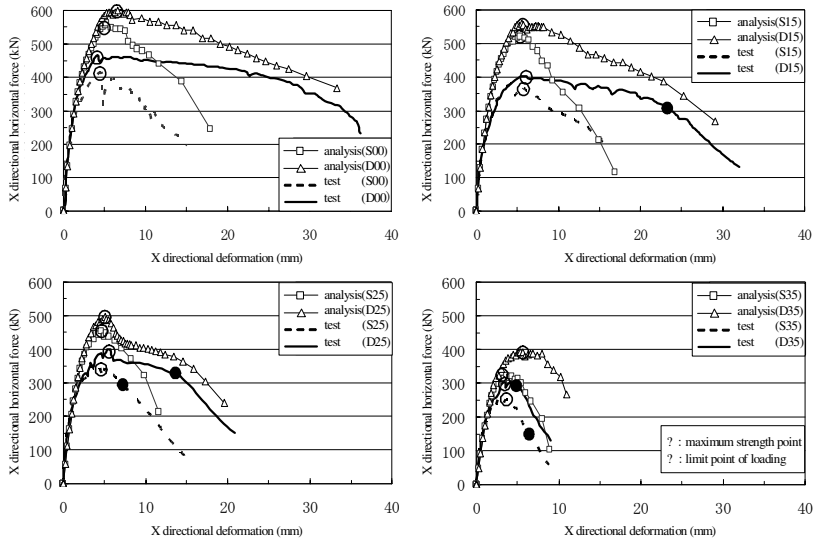


Fig.12 Relationship between X Directional Horizontal Force and X Directional Deformation

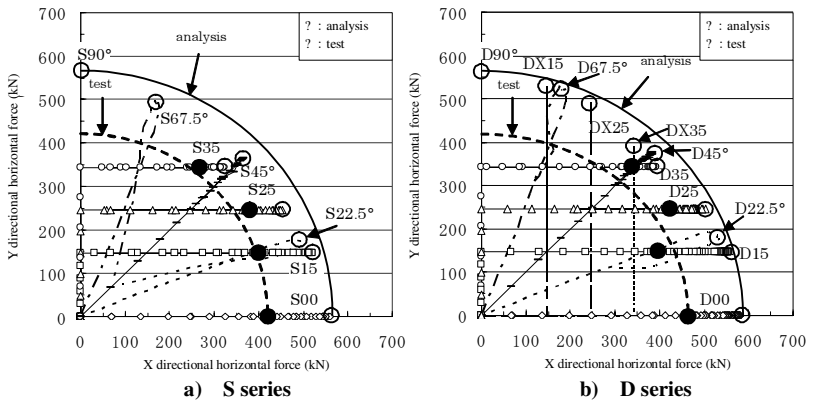


Fig.13 Relationship between X Directional Horizontal Force and Y Directional Horizontal Force

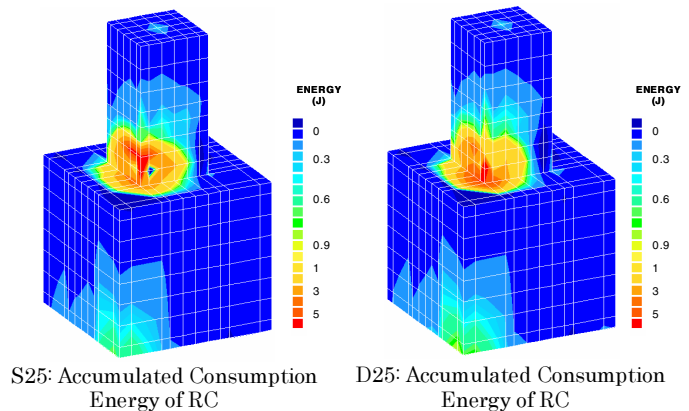


Fig.14 Accumulated Consumption Strain Energy of Specimens

### 3.3 Biaxial Failure Criteria

The relationships of Y directional horizontal force and X directional horizontal force of S series and D series are shown in Fig.13. In Fig.13.a), the circle which designates the maximum strength of specimen S00 as a radius, In Fig.13.b), the ellipse which designates the maximum strength of specimen D00 as a long axis, the maximum strength of specimen S00 as a short axis is drawn. The analytical result is shown on the solid line, and the experimental result is shown as a dotted line. The experimental maximum strength of each specimen is located on the circle or ellipse as the dotted line. However, the analytical strength deviates from the circle or ellipse as the solid line, and it locates in the inside vicinity of the circle. It is considered that the Y directional deformation increases, when the Y directional horizontal force is large. It is considered that X directional maximum strength of each specimen reaches earlier to the biaxial failure criteria, which is shown in Fig.13, from the damage at large deformation under the advanced Y directional loading.

### 3.4 Accumulated Consumption Strain Energy of Reinforced Concrete

The accumulated consumption strain energy of specimens S25 and D25 at the maximum strength is shown in Fig.14 for reinforced concrete. In this figure, it is recognized that the strain energy is intensive on the corner section of the compression side. As the future subject, it is necessary to consider the performance evaluation method and how to define the degree of damage by making use of accumulated consumption strain energy.

## 4. THREE-DIMENSIONAL FEM ANALYSIS OF RC BEAM-COLUMN JOINTS SUBJECTED TO BIAXIAL LOADING

### 4.1 Outline of Analysis

The specimen J-12, beam-column joint with lateral beams and slabs was tested by Shiohara (1993) [14]. The dimension and reinforcement arrangement of the specimen J-12 are shown in Fig.15. The material property is shown in Table.3. The specimen J-12 is a 1/2.5 scaled three-dimensional slab-beam-column joint. The beam span is 2,700mm, and the interstory height is 1,400mm. The dimensions of the beam and column are 30cm x 30cm and 24cm x 32cm, respectively. The thickness of slabs is 6cm. In the test, reversed cyclic loads were applied to two beam-ends of the specimen, with a constant axial force of 1590kN ( $=0.30 \sigma_B$ ) on the top. Loading patterns of horizontal force are shown in Fig.16. The drift angle R is 1/200, 1/100, 1/50, 1/33 and 1/25rad. The beam flexural yielding before joint shear failure was observed at R=1/33rad in the test. Therefore, the failure mode of the specimen was considered as the beam flexural yielding.

Fig.17(a) shows the modeling of the specimen J-12. In the analysis one and two directional lateral loads were given with monotonic increasing load. The concrete and reinforcement material property are the same as the experiment.

### 4.2 Analytical Results

#### 4.2.1 Story shear force-story displacement relationships

The analytical story shear force-story displacement relationships in two cases of one and two directional loading are shown as compared with the test results in Fig.18. The analytical initial stiffness was higher than the experiment. It is considered that this is due to the local flexural crack on the critical section of the beam and also neglecting the bond-slippage behavior between beam longitudinal bars and concrete in the joint. The analytical maximum story shear force of 404kN of one directional loading was higher than the test results of 370.7kN about 8.2%. In the analysis as well as the experiment, the beam flexural yielding before joint shear failure was observed both in one and two directional loading.

#### 4.2.2 Accumulated consumption strain energy of reinforced concrete

The accumulated consumption strain energy at the maximum strength of specimen J12 is shown in Fig.19. In the figure, it is recognized that the tensile energy of the concrete is about 1/100 times in comparison with compression side. In addition, from the vertical section of the beam main reinforcement position, the strain energy of tensile reinforcement was recognized. It is observed that the strain energy distribution of the joint becomes asymmetric in the top and bottom. Because of the slab, the energy of tensile reinforcement side where the slab is not attached is larger than the energy of tensile reinforcement side where the slab is attached. And the beam main reinforcement of the joint works as a truss mechanism, and the strain energy is stored there. Therefore, the energy of tensile reinforcement side where slab is not attached in joint is higher. The RC energy of compression side is observed, but there is a difference of energy of 50 times or more in comparison with the tensile side.

Compared with two directional loading, the stress is remarkable at one side of the beam in the case of one directional loading. Therefore, the energy of tensile side is larger. But, as for two directional loading, it is recognized that the energy in the joint is widely accumulated. In the future, it is necessary to consider the performance evaluation method and how to define the degree of damage by making use of the accumulated consumption strain energy.

Table.3 Material Properties

Specimen		J-12
(a) Beam	Section	24cm × 32cm
	Upper Bars	10-D 13
	Bottom Bars	10-D 13
	Shear Reinforcement	2-D 6@ 50
(b) Column	Section	30cm × 30cm
	Main Reinforcement	20-D 16
	Shear Reinforcement	3-D 6@ 50
(c) Joint	Shear Reinforcement	2-D 6 × 5 @ 50
(d) Slab	Type of Reinforcement	SD 35
	Bar Arrangement	D 6@ 150S

Specimen	Reinforcement	Yield Strength(MPa)	Tensile Strength(MPa)
J-12	USD685 D13	711	949
	USD980 D16	973	1058
	USD780 D6	800	950
	SD345 D6	399	501

Compressive Strength of Concrete	J-12 $\sigma_b = 60(\text{MPa})$
----------------------------------	----------------------------------

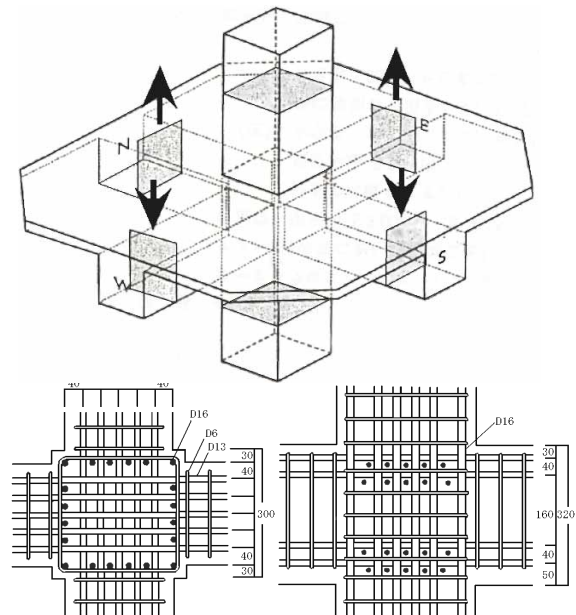


Fig.15 Dimension and Reinforcement Arrangement of Specimen J-12

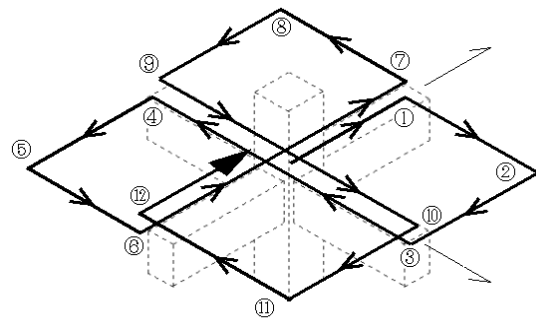


Fig.16 Loading Patterns

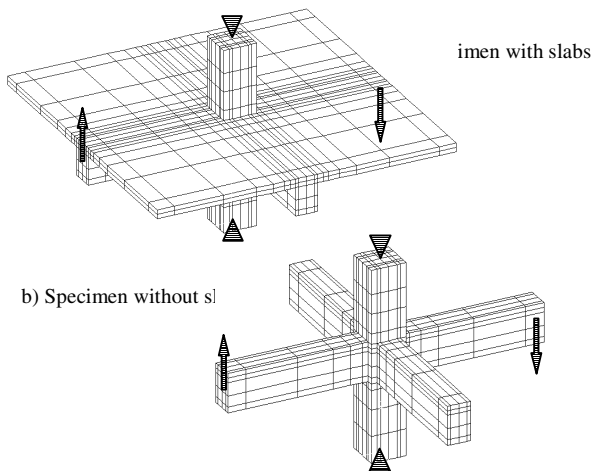


Fig.17 Finite Element Idealization and Boundary Condition

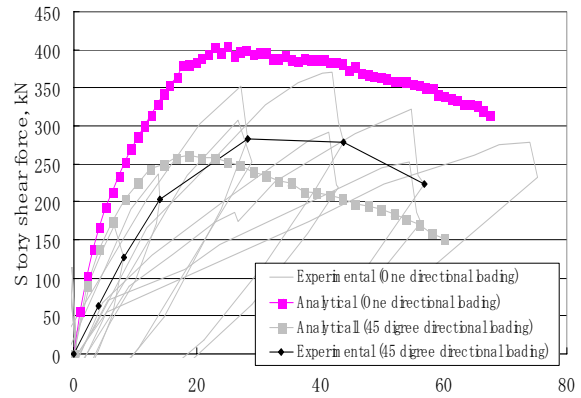


Fig.18 Story Shear Force-Story Displacement Relationships

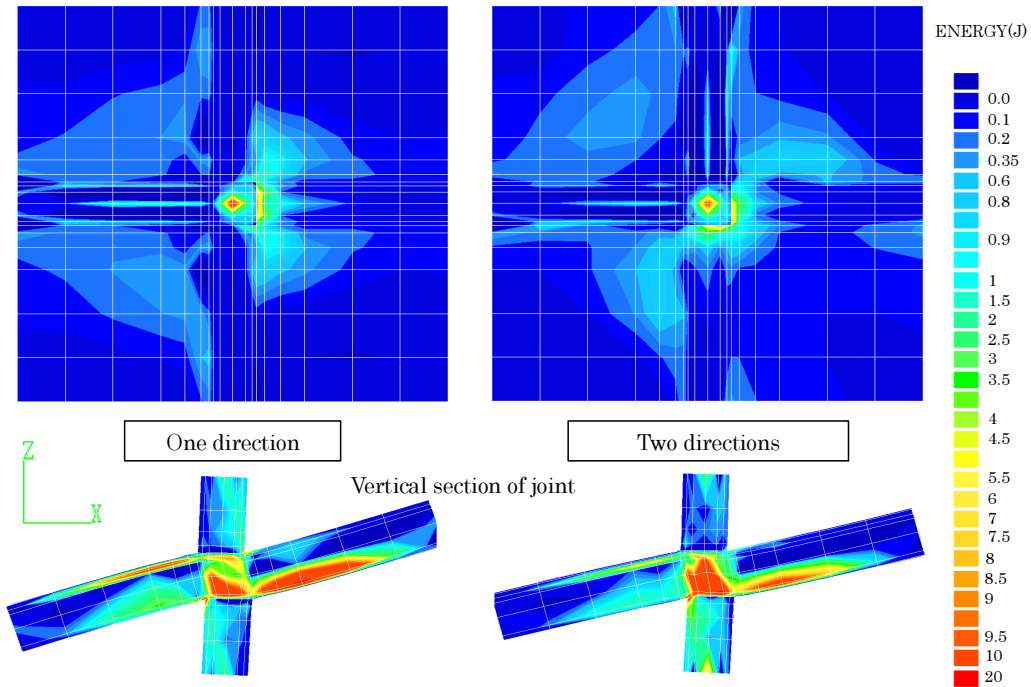


Fig.19 Distribution of Accumulated Consumption Strain Energy of Specimens

## 5. THREE-DIMENSIONAL FEM ANALYSIS OF RC BEAM-COLUMN JOINTS SUBJECTED TO REVERSED CYCLIC LOADINGS

RC beam-column joints with slabs were analyzed using the developed 3-D nonlinear FEM program in the case of reversed cyclic loading. The objectives are verification of the FEM program and investigation of the capability of predicting the hysteretic load-deformation behavior and evaluating the strain energy.

## 5.1 Outline of Analysis

As the objective specimens, five specimens, SU60, SU10, SU20, SU20N and BB20 were selected as beam-column joints with slabs subjected to one directional loading. One specimen BB20 is a beam-column joint without slabs subjected to two directional loading. Although specimen BB20 received two directional loading in the experiment, it received one directional loading in the analysis and compared with the experimental results of BB20. These specimens were tested by Suzuki (1984) [15]. Specimen BB20 excluded slabs of specimen SU20. Specimen BB20 has equivalent top beam bar and slab reinforcement quantity of specimen SU20. The number of specimen's name means axial force,  $\text{kgf/cm}^2$ . In specimen SU20N the shear reinforcement of the column, the beam and the joint was increased in comparison with specimen SU20.

Specimen Details and Material Properties are shown in Table.4. The finite element idealization and boundary condition are shown in Fig.17(a) and Fig.17(b). The column inflection point distance of the specimen is 1470mm, and the beam inflection point distance is 2700mm. As for the experimental loading method, after the axial force loading, the horizontal force was loaded at the top of the column. But in the analysis the anti-symmetrical vertical direction loads were added to the beam ends. In regard to the loading pattern, one cycle loading was done for each displacement unlike the experiment.

## 5.2 Analytical Results

### 5.2.1 Story shear force-story displacement relationships

The analytical story shear force-story displacement relationship of each specimen is shown as compared with the test results in Fig.20. Furthermore, the histeresis curves are compared in the case of perfect bond and normal bond for the beam bars in the joint. The analytical initial stiffness is higher than the experiment. It is considered that this is due to the opened crack at the critical section of the beam, which is not taken into account in the model.

In the experiment of specimen SU60 whose axial force is large, the slip characteristics are shown when the story displacement is 32mm. In the analysis of specimen SU60, in case of perfect bond, the slip characteristics are not observed to the last cycle, but, in the case of normal bond, the slip characteristics are observed when the story displacement is 32mm.

Table.4 Material Properties

Specimen		SU60	SU10	SU20	SU20N							
Column	Section( $\text{mm}^2$ )	300×300										
	Main Reinforcement	16-D10	16-D10	8-D13	12-D10							
	Shear Reinforcement	4-D6@50	4-D6@50	2-D6@50	4-D6@50							
Beam	Section( $\text{mm}^2$ )	200×300										
	Main Reinforcement	3-D13	3-D13	4-D13	3-D13							
	Shear Reinforcement	2-D6@50	2-D6@50	2-D6@80	2-D6@50							
Joint	Shear Reinforcement	4-D6@34	4-D6@34	2-D6@37.5	4-D6@23.3							
Slab	Thickness(mm)	70										
	Bar Arrangement	D6-@200	D6-@200	D6-@200	D6-@140							
Concrete(Column under slab, Beam, Slab)												
Secant Modulus of Elasticity ( $10^5 \text{N/mm}$ )		2.55	2.27	1.87	2.51							
Compressive Strength of Concrete ( $\text{N/mm}^2$ )		23.4	21.6	17.8	34.5							
Compressive Strength of Stress(%)		0.24	0.26	0.22	0.25							
Tensional Strength of Concrete ( $\text{N/mm}^2$ )		2.36	2.57	1.39	2.01							
Character of the Reinforcement												
Sort of Reinforcement		D6	D10	D13	D6	D10	D13	D6	D10	D13		
Yield Strength( $\text{N/mm}^2$ )		380	375	394	380	375	394	333	352	342	399	363

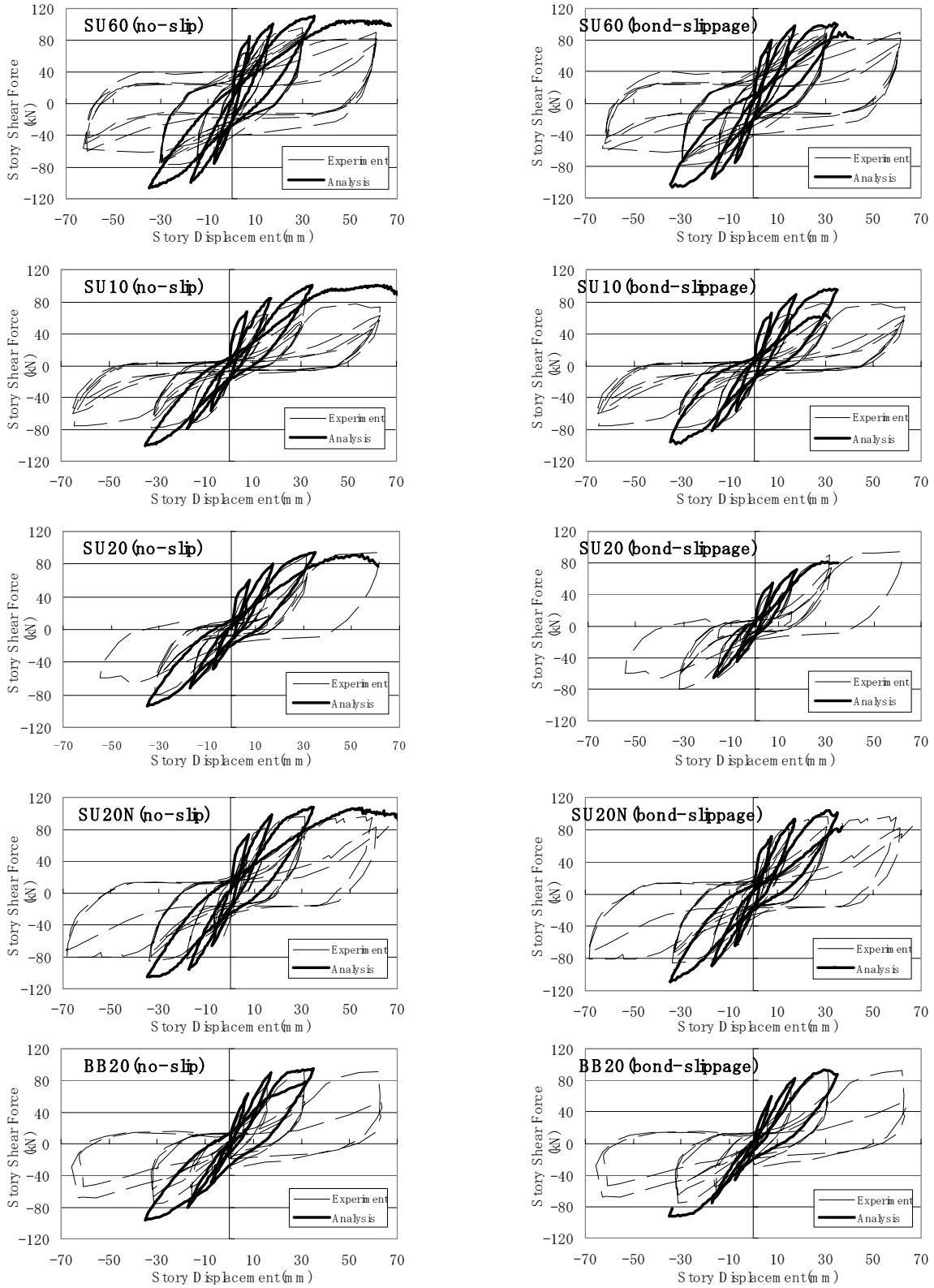


Fig.20 Story Shear Force-Story Displacement Relationships

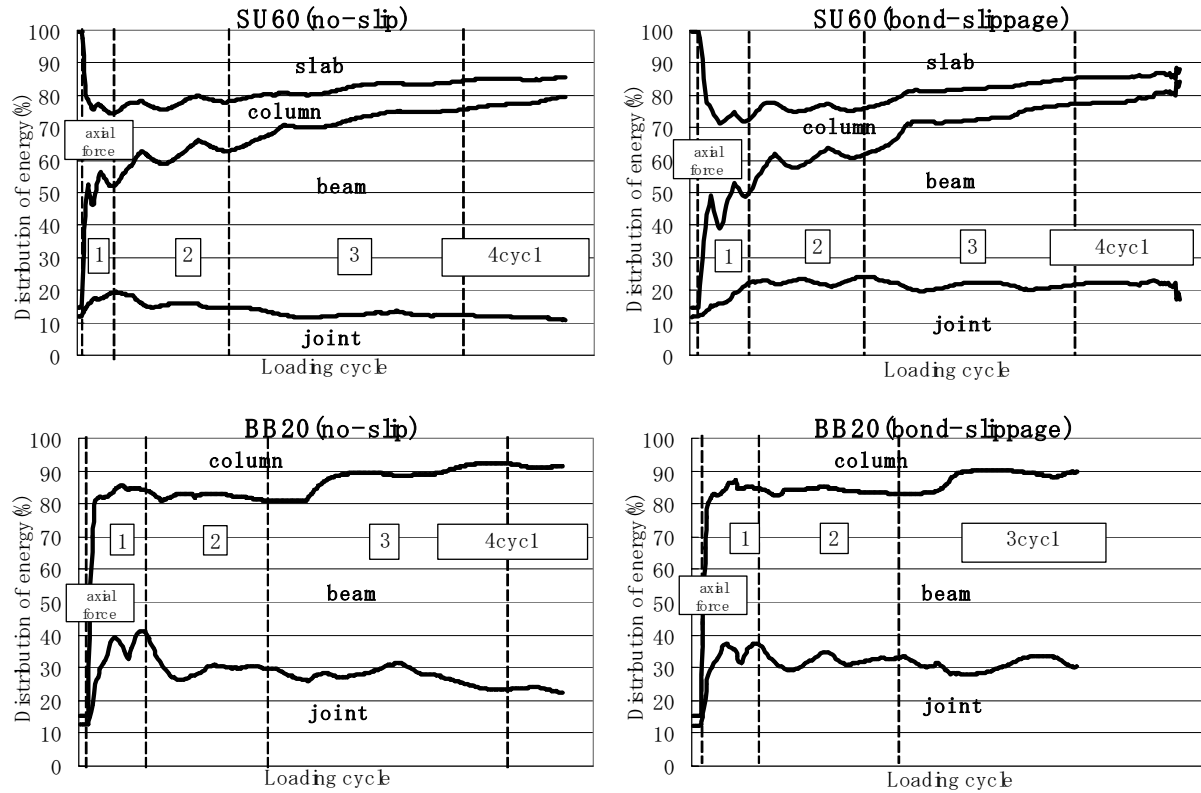


Fig.21 Distribution of Accumulated Consumption Strain Energy

In the experiment of specimen SU10 whose axial force is small, when the story shear force is about half of the maximum story shear force, the stiffness decreases suddenly. When the story displacement is 32mm, the specimen reaches the maximum strength, and when the story displacement is 64mm, the maximum story shear force is maintained. The analytical maximum story shear force is higher than the test results about 20%.

In the experiment of specimen SU20, which has the same hysteresis form of specimen SU10, when the story shear force is about half of the maximum story shear force, the stiffness decreases suddenly. When the story displacement is 32mm, the specimen reaches the maximum strength, and when the story displacement is 64mm, the maximum story shear force is maintained. In the analysis of SU20, in the case of both perfect bond and normal bond, when the story shear force is about half of the maximum story shear force, the stiffness decreases suddenly, and it is corresponding to the result. As for the maximum force, in the case of perfect bond, when the story displacement is 54mm, the maximum story shear force is not maintained, and the strength decreases. It is considered that the maximum force in the 3rd cycle is corresponding to the test result. In the analysis which considers the normal bond, because the analysis is stopped without convergence in the middle of the 3rd cycle. It is not possible to verify the quality of the slip characteristics.

As for the experimental value of specimen SU20N with heavier shear reinforcement than SU20, when story displacement is 16mm, the analytical strength of specimen SU20N is higher than the experimental value of SU20, after the story displacement exceeds 32mm. Although it shows the slip characteristics, the hysteresis area is still large. As compared with specimen SU20 whose shear reinforcement ratio was small, the stiffness and strength become large in all cycles. As for the analytical value of specimen SU20N,

compared with the perfect bond, the specimen with normal bond corresponds with the experimental results well.

The experimental results of specimen BB20 shows a similar behavior to specimen SU20. The analytical results of specimen BB20 shows similar behavior for both cases for bond conditions.

In the analysis which considers normal bond, each specimen has lower stiffness before unloading and higher stiffness after unloading near the 3rd cycle peak.

### 5.2.2 Accumulated consumption strain energy

Member contribution ratios of accumulated consumption strain energy of specimen SU60 with slabs and axial force, and specimen BB20 without slab are shown in Fig.21 in the case of perfect bond and normal bond. The member contribution ratios are calculated for a column, a beam and a joint as a ratio of the whole specimens energy. The ratio of the accumulated consumption strain energy of the joint with the normal bond type to the energy of the whole specimen is more than the perfect bond type. Because the damage may becomes larger by inserting bond-elements in the joint. The damage of the joint is becomes large from that the absorbed energy of the bond element become large under the cyclic loading.

Specimen BB20, excluding the slab from SU20, and also considering the reinforcing effect of slabs, is increased for the number of beam main bars. As a result, the bond area becomes large, and bond stress is maintained to the elastic range. As the energy of the bond element is not large, it is considered that there is not so much difference between the perfect bond and normal bond for the strain energy ratio of the joint. As for the column and slab of specimen SU60, where the cycle becomes many, the ratio which is occupied in the entire damage becomes small, and the ratio of the accumulated consumption strain energy of the beam becomes large.

Accumulated consumption strain energy of specimen SU60 (perfect bond) at the 4th cycle (story displacement is 32mm) is shown in Fig.22(a). The accumulated consumption strain energy (vertical section at beam main reinforcement position) of specimen BB20 (perfect bond) at the 4th cycle (story displacement is 32mm) is shown in Fig.22(b). Because of the beam flexural yields type, the centralization of the strain energy is observed mainly in upper and bottom bars near the plastic hinge regions and also slabs.

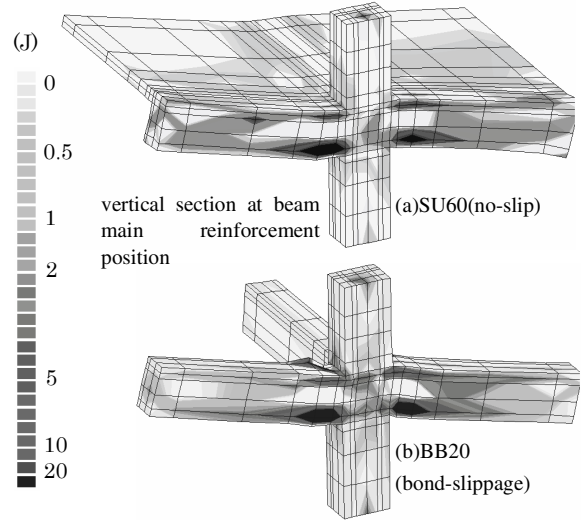


Fig.22 Accumulated Consumption Strain Energy (4th cycle)

## 6. CONCLUSIONS

In this study, in order to evaluate the damage process and the stress transfer mechanisms of reinforced concrete members under reversed cyclic loading, three-dimensional nonlinear FEM analysis program is developed. The columns and beam-column joints were analyzed in order to verify the revised analytical models. From the analytical results, it can be indicted that the behavior of RC members under reversed cyclic loading can be simulated precisely using the the reviced models.

## ACKNOWLEDGEMENTS

The work reported in this paper was sponsored by Grant-in Aid for Scientific Research (B) (2) (No. 14350293, Representative Researcher: Noguchi H., Chiba University) of the Ministry of Education, Culture, Sports and Science of Japanese Government. The authors wish to express their gratitude to Mr. Yu Y. of a graduate student, Messrs. Higashi R., Horibe A. and Sakamoto K. of former graduate students in Chiba University for their assistant on this study.

## REFERENCES

1. Uchida, K. and Noguchi, H. "Analysis of Two Story, Two Bay Frame Consisting of Reinforced Concrete Columns and Steel Beams with Through-Beam Type Beam-Column Joints." *Journal of Structural and Construction Engineering*; No.514; 207-214, (in Japanese), 1998.
2. Naganuma, K. & Ohkubo, M. "An Analytical Model For Reinforced Concrete Panels under Cyclic Stresses." *J. Struct. Constr. Eng., Architectural Institute of Japan*; No.536; 135-142, Oct., 2000
3. Ciampi, V. & Paolo, E. "Analytical Model for Concrete Anchorages of Reinforcing Bars under Generalized Excitations." Report No.UCB/ EERC-82/23. Earthquake Engineering Research Center, University of California, 1982.
4. Karsan, I. D. & Jirsa, J. O. "Behavior of Concrete under Compressive Loadings." *Journal of the Structural Division*; Vol.95; No.ST12: pp.2543-2563; American Society of Civil Engineers, 1969.
5. Tanigawa, Y. & Kosaka, Y. "Histeresis Model of Compression Area of Concrete." *Architectural Institute of Japan*; pp.449-450, 1978
6. Sato, T. & Shirai, N. "Elastic-Plastic Behavior of RC Shear Walls." *Summaries of Technical Papers of Annual Meeting C-2*; pp.1615-1618; Architectural Institute of Japan, 1978.
7. Ihzuka, T. & Noguchi, H. "Nonlinear Finite Element Analysis of Reinforced Concrete Members with Normal to High Strength Materials." *Proceedings of the Japan Concrete Institute*; Vol.14; No.2; pp.9-14; Japan Concrete Institute, 1992.
8. Kupfer, H. B. & Gerstle, K. H. "Behavior of Concrete under Biaxial Stresses." *Journal of the Engineering Mechanics Division*; American Society of Civil Engineers; Vol.99; No.EM4; pp.853-866, 1973.
9. Al-Mahaidi, R. S. H. "Nonlinear Finite Element Analysis of Reinforced Concrete Deep Members." Report No.79-1; Department of Structural Engineering, Cornell University; 1979.
10. Saenz, L. P. Discussion of "Equation for the Stress-Strain Curves of Concrete" by Desayi and Krishnan. *Proceedings of American Concrete Institute*; Vol.61, No.9: pp1229-1235; American Concrete Institute, 1964.
11. Uomoto, T., Yajima, T., and Hongo, K. "Damage evaluation of reinforced concrete beams subjected to cyclic bending moment using dissipated energy." *Summaries of Technical Papers of Annual Meeting of Japan Society of Civil Engineers*; No.460/V-18: 85-91, 1993.
12. Suzuki, M., Akakura, Y., Adachi, H., and Ozaka, Y. "Evaluation of damage index of reinforced concrete structure." *Summaries of Technical Papers of Annual Meeting of Japan Society of Civil Engineers*; No.490/V-23: 121-129, 1994.
13. Yoshimura, M., Tanaka, S., Suzuki, M. "Collapes of RC Columns Subjected to Earthquake Motions." *Proceedings of the Japan Concrete Institute*; Vol.14, No.2: pp.9-14: Japan Concrete Institute, 1998.
14. Shiohara, H. et al.. Evaluation of Slab-Beam-Column Joints Subjected to Bidirectional Loading(Part1,Part2,part3): *Architectural Institute of Japan* pp.877-882, 1993.9
15. Suzuki, N., Joshie K, H., Otani, S., and Aoyama, H. "Behaviour of Reinforced Concrete Beam-Column Subassemblages with and without Slab." Department of Architecture, Faculty of Engineering The University of Tokyo, 1984.
16. Architectural Institute of Japan; Design Guidelines for Earthquake Resistant Reinforced Concrete Buildings Based on Ultimate Strength Concept, 1990.

17. Architectural Institute of Japan; Design Guidelines for Earthquake Resistant Reinforced Concrete Buildings Based on Ultimate Strength Concept: Architectural Institute of Japan, 1990.
18. Architectural Institute of Japan; Design Guidelines for Earthquake Resistant Reinforced Concrete Buildings Based on Inelastic Displacement Concept. Architectural Institute of Japan, 1999.
19. Stevens, N. J., Uzumeri, S. M. & Collins, M. P. "Analytical Modeling of Reinforced Concrete Subjected to Monotonic and Reversed Loadings." Publication No.87-1. Department of Civil Engineering, University of Toronto, 1987.
20. Sakurai, T., Kashiwazaki, T., and Noguchi, H. "Development of Nonlinear FEM Analytical Models for RC Membranes Subjected to Reversed Cyclic Loading." Proceedings of the Japan Concrete Institute; Vol.24; No.2; pp.139-144; Japan Concrete Institute, 2002.